S-Alkylation-Induced Redox Reactions Leading to Reversible Sulfur−Sulfur Coupling in a Pentamethylcyclopentadienyl Ruthenium(III) Thiolate-Thioether System†

Richard Yee Cheong Shin, Ming Ern Teo, Weng Kee Leong, Jagadese J. Vittal, John Hon Kay Yip, and Lai Yoong Goh*

Department of Chemistry, National University of Singapore, Kent Ridge, Singapore 117543

Richard D. Webster*

Research School of Chemistry, Australian National University, Canberra, ACT 0200, Australia

Received November 25, 2004

Alkylation of [Cp*Ru^{III}(tpdt)] (**2**) (Cp* = η^5-C_5Me_5, tpdt = η^3-$S(CH_2CH_2S^-)_2$) with MeI or Me_3OBF_4 resulted in the formation of a *trans* μ-η^1-η^1-S_2 coupled species, [{Cp*Ru^{II}}$_2${μ-η^6-$(S(CH_2)_2S(CH_2)_2SMe)_2$}]$^{2+}$ (**3**) as the predominant product. With MeI the reaction also gave a small amount of [Cp*Ru^{II}{η^3-$S(CH_2CH_2SMe)_2$}]I, **4**(I), but in the presence of acrylonitrile (AN), the products were **4**(I) and [Cp*Ru^{II}{η^3-$S((CH_2)_2S)_2(CH_2CHCN)$}]I, **5**(I), of which the latter was the sole product from the reaction of **2** with AN in the presence of iodine. **2** was electrochemically easily oxidized in a one-electron process; its chemical oxidation with I_2 led to the isolation of [{Cp*Ru^{II}}$_2${μ-η^6-$(S(CH_2CH_2S)_2)_2$}]$(I_3)_2$, **6**$(I_3)_2$, containing a cyclic $Ru^{II}(\mu$-$S_2)_2Ru^{II}$ core. A combination of electrochemical, EPR, UV−vis, and NMR experiments indicated that the solution phase chemistry of **3** is governed by its facile reversible dissociation into the mononuclear cation radical (**3A**). Based on this phenomenon were rationalized the pathways leading to the formation of the dinuclear species [{Cp*Ru^{II}}$_2${μ-η^5-$MeS(CH_2)_2$-$S(CH_2)_2SS(CH_2)_2S(CH_2)_2S$}]$^+$ (**7**) from the interaction of **3** and **2**, or of a mixture of **4**(I) and **5**(I) in the presence of MeI and AN, and of [Cp*Ru^{II}{η^3-$MeS(CH_2)_2S(CH_2)_2SSnBu_3$}]$^+$ (**9**) from reaction with tri(*n*-butyl)tin hydride. Electrochemical measurements indicated that the sodium naphthalide reduction of **3** to generate the mono-S-methylated derivative, [Cp*Ru^{II}-{η^3-$S(CH_2)_2S(CH_2)_2SMe$}] (**8**), occurred through **3A**. It is proposed that some of the transformations also involved internal electron transfers and nucleophilic displacements. The X-ray crystal structures of the complexes **3**−**9** are reported.

Introduction

One of the salient reactivity features of *cis*-dithiolate complexes is their ability to undergo S-alkylation. In a methodology developed by Busch, dialkylation by α,ω-alkyldihalides has been used to template the synthesis of thioether macrocycles at Ni(II) centers;[1] subsequently the method has been utilized by Sellmann for the synthesis of 1,4,7-trithiacyclononane (9S3) via a Mo(9S3) complex[2] and extensively by Darensbourg[3] for the synthesis of macrocyclic N_2S_2 and N_3S_2 donor ligand sets via precursor complexes of Ni(II), Co(II), and Rh(III). In recent studies, we have similarly prepared several mesocyclic (*z*S3, *z* = 8−12) complexes of (arene)Ru(II) from [(HMB)Ru(tpdt)] (**1**) (HMB = η^6-C_6Me_6, tpdt = η^3-$S(CH_2CH_2S^-)_2$) and also found that the use of monofunctional methyl iodide resulted in sequential mono- and di-S-alkylation (Scheme 1).[4] Unexpectedly preliminary findings showed that a similar reaction of the Ru(III) complex [Cp*Ru(tpdt)] (**2**) (Cp* = η^5-C_5Me_5) led to alkylation at one S atom and S−S coupling at the other, yielding the Ru(II) complex **3** as the predominant product (eq i).[5] It is apparent that there had occurred a −1 oxidation state change at Ru. There are ample examples of redox processes in which an external *oxidant* has resulted in reduction at the metal center, from the work of Taube[6] and Deutsch[7] in Co(III) ammine chemistry, and the work of Stiefel on the tetrachalcogenometalates of V, Mo and W, and Re.[8]

Scheme 1

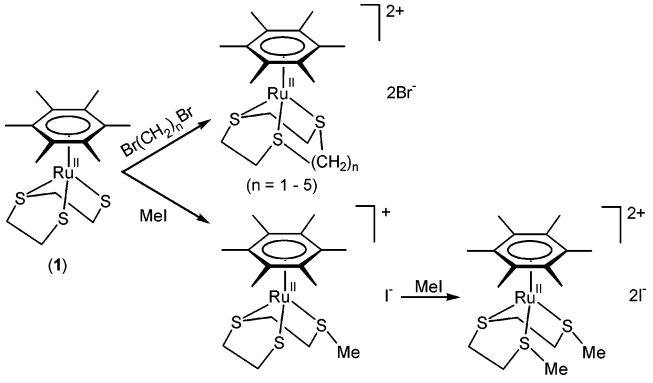

† In honor of Prof. Martin A. Bennett.

* To whom correspondence should be addressed. Fax: (+65) 6779 1691. E-mail: chmgohly@nus.edu.sg; webster@rsc.anu.edu.au.

(1) Thompson, M. C.; Busch, D. H. *J. Am. Chem. Soc.* **1964**, *86*, 3651.

(2) Sellmann, D.; Zapf, L. *J. Organomet. Chem.* **1985**, *289*, 57.

(3) Goodman, D. C.; Reibenspies, J. H.; Goswami, N.; Jurisson, S.; Darensbourg, M. Y. *J. Am. Chem. Soc.* **1997**, *119*, 4955, and references therein.

10.1021/om049081o CCC: $30.25
Publication on Web 02/26/2005

However, such alkylation-induced redox processes resulting in S−S coupling have not been reported before.

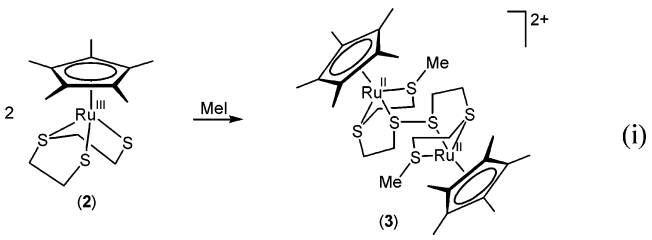

(i)

In view of the high level of interest in the involvement of disulfide bonds in biological and industrial processes,[9,10] we have carried out an in-depth investigation of the mechanism of this reaction. Disulfide bond formation in coordination and organometallic compounds and in the tertiary structure of many proteins has been established to occur by oxidative coupling.[11] The first example was Taube's synthesis of the $[(L_5Ru)_2(\mu\text{-}S_2)]^{n+}$ diruthenium(III) species **A** by oxidation of $[(L_5Ru^{II}X)]^{2+}$ ($X = H_2S$ or SH, $L = NH_3$) with air or oxygen.[12] Subsequently, other μ-S_2 dinuclear analogues possessing variants in L_5 were similarly obtained by Rauchfuss,[13] Sellmann,[14] and Puerta.[15] In general, disulfides are easily activated by reductive cleavage, both chemically and electrochemically.[16a,b] However, recent studies have revealed diverse cleavage pathways, including, for instance, dissociative electron transfer proceeding through formation of radical anion species[16b−d] and reversible redox activation of S−S bonds in enzymatic species.[16e]

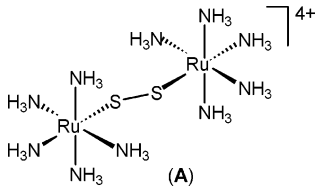

(**A**)

The results of this present study revealing a new pathway for the formation and cleavage of S−S bonds in ruthenium complexes will be described in this paper.

Experimental Section

General Procedures. All general procedures and the preparation of [Cp*Ru(tpdt)] (**2**) were as previously described.[17] Methyl and ethyl iodides, 2-mercaptoethyl sulfide, acrylonitrile, tri(*n*-butyl)tin hydride, and trimethyloxonium tetrafluoroborate were obtained from Aldrich and used as supplied.

Cyclic voltammetry (CV) experiments were conducted with a computer-controlled Eco Chemie μAutolab III potentiostat using a 1.0 mm diameter glassy carbon (GC) working electrode in conjunction with a Pt wire auxiliary electrode and an Ag wire reference electrode. The electrochemical cell was jacketed in a glass sleeve and cooled to 233 K, using a Lauda variable-temperature methanol-circulating bath.

Solutions of electrogenerated compounds for the EPR experiments were prepared at 233 K in a divided controlled potential electrolysis cell and then transferred under vacuum into cylindrical 3 mm (i.d.) EPR tubes that were immediately frozen in liquid N_2. EPR spectra were recorded on a Bruker ESP 300e spectrometer in a TE_{102} cavity at 10 K using liquid He cooling and at temperatures between 293 and 193 K using liquid N_2 cooling.

(a) Reaction of 2 with Methylating Agents. (i) With Methyl Iodide. To a dark purple solution of **2** (50 mg, 0.13 mmol) in toluene (15 mL) was added MeI (80 μL, 1.28 mmol) with stirring. Precipitation was observed immediately. After stirring for 1 h, the reaction mixture was evacuated to dryness and the red residue recrystallized in MeOH/ether. Red needle-shaped crystals of $[\{Cp^*Ru\}_2\{\mu\text{-}\eta^6\text{-}(S(CH_2)_2S(CH_2)_2SMe)_2\}](I)_2$, $\mathbf{3}(I)_2$ (52 mg, 76% yield), were obtained after 24 h at −30 °C. Upon removal of solvent, the mother liquor gave a noncrystallizable oil, the proton NMR and mass spectra of which showed the presence of a mixture of species **3** and $[Cp^*Ru\{\eta^3\text{-}S(CH_2CH_2SMe)_2\}]^+$ (**4**), which is characterized as described below. Diffraction-quality crystals of $\mathbf{3}(I)_2$ were obtained by diffusion of ether into an acetonitrile solution for 2 weeks at −30 °C. Anal. Calcd (Found) for $\mathbf{3}(I)_2 \equiv (C_{30}H_{52}I_2Ru_2S_6)$: C, 34.0 (33.9), H, 4.9 (4.8), S, 18.1 (18.0).

A solution of $\mathbf{3}(I)_2$ (20 mg, 0.02 mmol) in methanol (ca. 8 mL) was treated with excess NH_4PF_6 (15 mg, 0.09 mmol) to precipitate the product as a dark red-brown solid. Extraction of this with CH_3CN gave a dark red solution, which upon concentration and addition of ether gave fine red microcrystals of $\mathbf{3}(PF_6)_2$ (19 mg, 92% isolated yield).

(4) Shin, R. Y. C.; Bennett, M. A.; Goh, L. Y.; Chen, W.; Hockless, D. C. R.; Weng, W. K.; Mashima, K.; Willis, A. C. *Inorg. Chem.* **2003**, *42*, 96.

(5) Teo, M. E. MSc Thesis, Department of Chemistry, National University of Singapore, 2001.

(6) Taube, H. *Electron-Transfer Reactions of Complex Ions in Solution;* Academic Press: New York, 1970; Chapter 4, pp 73−98, and references therein.

(7) (a) Woods, M.; Karbwang, J.; Sullivan, J. C.; Deutsch, E. *Inorg. Chem.* **1976**, *15*, 1678. (b) Nosco, D. L.; Elder, R. C.; Deutsch, E. *Inorg. Chem.* **1980**, *19*, 2545. (c) Lydon, J. D.; Elder, R. C.; Deutsch, E. *Inorg. Chem.* **1982**, *21*, 3186.

(8) (a) Coyle, C. L.; Harmer, M. A.; George, G. N.; Daage, M.; Stiefel, E. I. *Inorg. Chem.* **1990**, *29*, 14, and references therein. (b) Murray, H. H.; Wei, L.; Sherman, S. E.; Greaney, M. A.; Eriksen, K. A.; Carstensen, B.; Halbert, T. R.; Stiefel, E. I. *Inorg. Chem.* **1995**, *34*, 841, and references therein.

(9) (a) Mùller, A., Krebs, B., Eds. *Sulfur−Its Significance for Chemistry; for the Geo-, Bio-, and Cosmosphere and Technology*; Elsevier: Amsterdam, 1984. (b) Stiefel, E. I., Matsumoto, K., Eds. *Transition Metal Sulfur Chemistry: Biological and Industrial Significance*; ACS Symposium Series No. 653; American Chemical Society: Washington, D.C., 1996. (c) Weber, T., Prins, R., van Santen, R. A., Eds. *Transition Metal Sulphides: Chemistry and Catalysis*; NATO ASI series Vol. 60; Kluwer Academic Publishers: Dordrecht, 1998. (d) Stiefel, E. I., Coucouvanis, D., Newton, W. E., Eds. *Molybdenum Enzymes, Cofactors, and Model Systems*; ACS Symposium Series No. 535; American Chemical Society: Washington, D.C., 1993.

(10) See, for instance, the following and references therein: (a) Rabenstein, D. L.; Yeo, P. L. *J. Org. Chem.* **1994**, *29*, 26 (on peptide hormones). (b) Kim, J.; Rees, D. C. *Science* **1992**, *257*, 1677 (on P-cluster of the nitrogenase enzyme). (c) Dai, S.; Schwendmayer, C.; Schürmann, P.; Ramaswamy, S.; Eklund, H. *Science* **2000**, *287*, 655 (on determinant of conformations/shapes of proteins). (d) Barbitz, S.; Jacob, U.; Glocker, M. O. *J. Biol. Chem.* **2000**, *275*, 18759 (on chaperon activities of disulfide isomerases). (e) Baker, A.; Payne, C. M.; Briehl, M. M.; Powis, G. *Cancer Res.* **1997**, *57*, 5162, and references therein (on cell growth and cancers).

(11) (a) Blower, P. J.; Dilworth, J. R. *Coord. Chem. Rev.* **1987**, *76*, 121. (b) Deutsch, E.; Root, M. J.; Nosco, D. L. *Adv. Inorg. Bioinorg. Mech.* **1982**, *1*, 269, and references therein. (c) Frausto da Silva, J. J. R.; Williams, R. J. P. *The Biological Chemistry of the Elements*; Clarendon: Oxford, 1991; pp 164−170.

(12) (a) Kuehn, C. G.; Taube, H. *J. Am. Chem. Soc.* **1976**, *98*, 689. (b) Elder, R. C.; Trkula, M. *Inorg. Chem.* **1977**, *16*, 1048.

(13) (a) Amarasekera, J.; Rauchfuss, T. B.; Wilson, S. R. *Inorg. Chem.* **1989**, *28*, 3875. (b) Amarasekera, J.; Rauchfuss, T. B.; Wilson, S. R. *Inorg. Chem.* **1987**, *26*, 3328.

(14) Sellmann, D.; Lechner, P.; Knoch, F.; Moll, M. *J. Am. Chem. Soc.* **1992**, *114*, 922.

(15) Coto, A.; Tenorio, M. J.; Puerta, M. C.; Valerga, P. *Organometallics* **1998**, *17*, 4392.

(16) See for instance: (a) Alfassi, Z. B., Ed. *S-Centered Radicals*; Wiley: Chichester, 1999. (b) Antonello, S.; Benassi, R.; Gavioli, G.; Taddei, F.; Maran, F. *J. Am. Chem. Soc.* **2002**, *124*, 7529. (c) Daasbjerg, K.; Jensen, H.; Benassi, R.; Taddei, F.; Antonello, S.; Gennaro, A.; Maran, F. *J. Am. Chem. Soc.* **1999**, *121*, 1750. (d) Antonello, S.; Daasbjerg, K.; Jensen, H.; Taddei, F.; Maran, F. *J. Am. Chem. Soc.* **2003**, *125*, 14905. (e) Wang, D.; Behrens, A.; Farahbakhsh, M.; Gatjens, J.; Rehder, D. *Chem. Eur. J.* **2003**, *9*, 1805.

(17) Goh, L. Y.; Teo, M. E.; Khoo, S. B.; Leong, W. K.; Vittal, J. J. *J. Organomet. Chem.* **2002**, *664*, 161.

Data for 3(PF$_6$)$_2$: ^{1}H NMR (300 MHz, CD_2Cl_2): at 298 K, δ 1.73, 1.41, and 1.14 ($\nu_{1/2}$ 70, 50, and 70 Hz; relative intensity ca. 1:2:1) and at 213 K, δ 1.65, 1.59 (each s, C_5Me_5), and very broad resonances for SCH_2 and SCH_3 (total 22 H's) as follows: δ 3.27 (cm unres, 4H), δ 3.08 (cm unres, 2H), δ 3.00−2.45 (numerous small peaks, 2H), δ 2.39, 2.35, 2.30, and 2.29 sitting on a broad band centered at δ 2.33 (6H), δ 2.08 (cm unres, 3H); δ 1.78 (c of broad "bands", 2H), and δ 1.47 (c of broad band, 2H). A variable-temperature stacked plot is given in Figure 3. IR (ν cm^{-1}, KBr): (PF_6^-) 841vvs, 557vs. FAB$^+$ MS: *m/z* 404 [M − 2PF$_6$]$^{2+}$. FAB$^-$ MS: *m/z* 145 [PF$_6$]$^-$. Anal. Calcd (Found) for **3**(PF$_6$)$_2$ ≡ ($C_{30}H_{52}F_{12}P_2Ru_2S_6$.2$CH_3CN$): C, 34.6 (34.6); H, 5.0 (4.9); N, 2.4 (2.4); P, 5.3 (5.9); S, 16.3 (15.9).

A similar reaction with EtI is described in the Supporting Information.

(ii) With (Me$_3$O)BF$_4$. To a solution of **2** (20 mg, 0.05 mmol) in methanol (15 mL) was added (Me_3O)BF_4 (76 mg, 0.5 mmol) with stirring. An instantaneous color change from deep purple to dark red was observed. After stirring for 15 min, the solution was concentrated to half volume and ether added. Very fine brownish red needles of **3**(BF$_4$)$_2$ (17 mg, 67%) were obtained after 24 h at −30 °C. Anal. Calcd (Found) for **3**(BF$_4$)$_2$ ≡ ($C_{30}H_{52}B_2F_8Ru_2S_6$): C, 36.7 (36.2); H, 5.3 (5.4); S, 19.6 (19.8). The compound possesses ^{1}H NMR spectral features identical to those of the PF_6^- salt of **3** above. The proton NMR spectrum of the mother liquor showed no trace of **4**.

(iii) Estimate of Relative Reaction Rate of 2 with MeI and (Me$_3$O)BF$_4$. (a) With MeI. To a purple solution of **2** (5 mg, 0.01 mmol) in hexane (5 mL) was injected MeI (8 μL, 0.13 mmol) with stirring. The products started to precipitate after 10 min, and the solution slowly decolorized, turning almost colorless after 6 h. **(b) With (Me$_3$O)BF$_4$.** To a purple solution of **2** (5 mg, 0.01 mmol) in hexane (5 mL) was added (Me_3O)BF_4 (19 mg, 0.13 mmol) with stirring. Precipitation was observed immediately with the solution changing to very pale purple within 5 min and to colorless after 30 min. It was estimated that the reaction with (Me_3O)BF_4 was at least an order of magnitude faster than with MeI.

(b) Reaction of 2 with Methylation Agents in the Presence of Acrylonitrile (AN). (i) With MeI. Into a stirred deep purple solution of **2** (30 mg, 0.07 mmol) in CH_3CN (10 mL) was injected AN (45 μL, 0.68 mmol), followed by MeI (15 μL, 0.24 mmol). An instantaneous color change to yellow was observed. The reaction mixture was stirred for 1 h and then evacuated to dryness. The yellow residue was recrystallized in CH_3CN (ca. 1 mL) and ether, giving yellow orthorhombic-shaped crystals of [Cp*Ru{η^3-S($(CH_2)_2$S)$_2$(CH_2CHCN)}]I, **5**(I) (20 mg, 46% yield), after 3 days at −30 °C, followed by a second crop of yellow solids (17 mg) consisting of **5**(I) and **4**(I) in the ratio of 1:6 (equivalent to **5**(I) (5% yield) and **4**(I) (29% yield)), with more of **4** in the mother liquor. Diffraction quality crystals of **5**(I) were obtained by diffusion of ether into an acetonitrile solution for a week at −30 °C. There was no sign of the presence of compound **3** (see section d(ii) below for the rapid reaction of **3** with **2** in the presence of MeI and AN).

A repeat of this reaction in *hexane* gave reddish orange precipitates, consisting of an inseparable mixture of iodides of **3**, **4**, and **5** in a colorless supernatant.

Data for 4(I): ^{1}H NMR (δ, CD_3CN): 2.77−2.65 (8-line m, 4H, SCH_2), 2.48−2.36 (m unres, 2H, SCH_2), 2.20 (s, 6H, SMe), 2.13−2.03 (m unres, 2H, SCH_2), 1.71 (s, 15H, C_5Me_5). ^{13}C NMR (δ, CD_3CN): 89.9 (C_5Me$_5$), 38.5, 35.5 (SCH_2), 22.7 (SCH_3), 9.7 (C_5Me_5). FAB$^+$ MS: *m/z* 419 [M − I]$^+$, 389 [M − I − 2Me]$^+$. FAB$^-$ MS: *m/z* 127 [I]$^-$. HR-FAB$^+$ MS: *m/z* 419.0473 (found), 419.0469 (calcd). For microanalytical data see section (e) below.

Data for 5(I): ^{1}H NMR (δ, CD_3CN): 4.01 (t, 1H, CH), 2.81−2.71 (9-line m, 2H, SCH_2), 2.64−2.41 (15-line m, 8H, SCH_2), 1.81 (s, 15H, C_5Me_5). ^{13}C NMR (δ, $(CD_3)_2CO$): 117.8 (C≡N), 93.1 (C_5Me$_5$), 39.3, 37.2, 36.3, 35.0, 34.7 (SCH, SCH_2), 9.9 (C_5Me_5). ^{13}C NMR (δ, CD_3CN): 93.5 (C_5Me$_5$), 39.0, 37.2, 36.8, 36.1, 34.5, 34.3 (SCH, SCH_2), 9.9 (C_5Me_5). IR (ν cm^{-1}, KBr): 2244m (C≡N). FAB$^+$ MS: *m/z* 442 [M − I]$^+$, 389 [M − I − (CH_2CHCN)]$^+$. FAB$^-$ MS: *m/z* 127 [I]$^-$. HR-FAB$^+$ MS: *m/z* 442.0272 (found), 442.0265 (calc). Anal. Calcd (found) for **5**(I) ≡ ($C_{17}H_{26}INRuS_3$·CH_3CN): C, 37.4 (37.3); H, 4.8 (4.9); N, 4.6 (4.7); S, 15.8 (16.0).

(ii) With (Me$_3$O)BF$_4$. Into a stirred purple solution of **2** (22 mg, 0.056 mmol) in CH_3CN (5 mL) was injected AN (8 μL, 0.12 mmol), followed by (Me_3O)BF_4 (17 mg, 0.11 mmol). A very deep red coloration developed immediately. After stirring for 1 h, the product mixture was evacuated to dryness. The residue was then recrystallized in CH_3CN and ether, giving deep red needle-shaped crystals of **3**(BF$_4$)$_2$ (12 mg, 41%) after 1 day at −30 °C. Identification was by comparison of its ^{1}H NMR spectral data with that of **3**(I)$_2$. The ^{1}H NMR spectrum of the orange-red mother liquor shows the presence of a 1:1 molar mixture of **4** and **5**.

(c) Reaction of 2 with I$_2$. (i) To a stirred purple solution of **2** (16 mg, 0.04 mmol) in toluene (8 mL) was added solid I_2 (10.8 mg, 0.04 mmol). The solution underwent instantaneous decolorization with precipitation of brown solids. After stirring for 15 min the solids were filtered and washed with toluene (2 × 5 mL), followed by hexane (2 × 5 mL), and evacuated dry. Recrystallization in acetonitrile/ether gave fine brown needles of [{Cp*Ru}$_2${μ-η^6-(S(CH_2CH_2S)$_2$)$_2$}](I$_3$)$_2$, **6**(I$_3$)$_2$ (21 mg, 69% yield), after 24 h at −30°C.

Data for 6(I$_3$)$_2$: ^{1}H NMR (δ, CD_3CN): 3.82−3.74 (7-line m, 4H, SCH_2), 3.46−3.38 (7-line m, 4H, SCH_2), 3.35−3.26 (5-line m, 4H, SCH_2), 3.08−3.00 (7-line m, 4H, SCH_2), 1.67 (s, 30H, C_5Me_5). ^{13}C NMR (δ, CD_3CN): 106.1 (C_5Me$_5$), 43.8, 41.4 (SCH_2), 10.2 (C_5Me_5). FAB$^+$ MS: *m/z* 389 [M]$^{2+}$. Anal. Calcd (found) for **6**(I$_3$)$_2$ ≡ ($C_{24}H_{46}I_6Ru_2S_6$): C, 21.9 (21.6); H, 3.0 (3.2); S, 12.5 (12.5).

(ii) In the Presence of AN. Into a stirred deep purple solution of **2** (12 mg, 0.03 mmol) in CH_3CN (5 mL) was injected AN (15 μL, 0.23 mmol), followed by solid I_2 (16 mg, 0.06 mmol). The color changed instantaneously to yellow and then reddish as the unconsumed I_2 dissolved. After stirring for 30 min the solution was evacuated to dryness and the residue washed with toluene (3 × 2 mL) to remove excess I_2. The orange residual solids was recrystallized in acetonitrile/ether, giving brownish yellow crystals of **5**(I$_3$) (12 mg, 47%) after a day at −30 °C, followed by a second crop of golden brown plates of the same compound (4 mg, 16% yield) after 2 days. Anal. Calcd (found) for **5**(I$_3$) ≡ ($C_{17}H_{26}I_3NRuS_3$): C, 24.8 (25.1); H, 3.2 (3.1); N, 1.7 (1.6); S, 11.7 (11.0). The ^{1}H NMR and mass spectra matched those of **5**(I).

(d) S−S Bond Dissociation in 3. (i) Reaction of 3(I)$_2$ with 2. To a stirred dark red solution of **3**(I$_2$ (25 mg, 0.02 mmol) in CH_3CN (10 mL) was added solid **2** (20 mg, 0.05 mmol). After 12 h, the resulting dark brown solution was evacuated to dryness and the blackish oily residue triturated with toluene (3 × 3 mL) to extract the slight excess of **2** used. The residual solids were then recrystallized in CH_2Cl_2/ether to give dark reddish brown parallelepiped crystals of [{Cp*Ru}$_2$-{μ-η^5-MeS(CH_2)$_2$S(CH_2)$_2$SS(CH_2)$_2$S(CH_2)$_2$S}]I, **7**(I) (24 mg, 55% yield), after 3 days at −30 °C.

Data for 7(I). ^{1}H NMR (δ, CD_3CN): 3.61−3.54 (8-line m, 2H, SCH_2), 2.84−2.74 (10-line m, 2H, SCH_2), 2.71−2.52 (13-line m, 4H, SCH_2), 2.43−2.33 (9-line m, 2H, SCH_2), 2.24−2.09 (8-line m, 2H, SCH_2), 2.16 (s, 3H, SMe), 1.88−1.82 (5-line m, 1H, SCH_2), 1.72 (s, 15H, C_5Me_5), 1.70 (s, 15H, C_5Me_5), 1.63−1.48 (8-line m, 1H, SCH_2), 1.15−0.96 (11-line m, 1H, SCH_2), 0.60−0.50 (6-line m, 1H, SCH_2), 0.26−0.16 (7-line m, 1H, SCH_2). ^{13}C NMR (δ, CD_3CN): 94.0, 92.4 (C_5Me$_5$), 42.0, 38.4, 35.9, 35.7, 35.0, 34.0, 32.4, and 32.3 (SCH_2), 15.8 (SMe), 10.5, 10.4 (C_5Me_5). FAB$^+$ MS: *m/z* 793 [M + H]$^+$. Anal. Calcd (found) for **7**(I) ≡ ($C_{29}H_{49}IRu_2S_6$): C, 37.9 (37.8); H, 5.4 (5.5); S, 20.9 (21.4).

(ii) Reaction of 3(I)$_2$ with 2 in the Presence of MeI and AN. Into a stirred deep red suspension of **3**(I$_2$ (10 mg, 0.01 mmol), partially dissolved in CH_3CN (10 mL), was injected AN

(30 μL, 0.46 mmol), followed by MeI (15 μL, 0.24 mmol). No change was observed after stirring for 1 h (a prolonged reaction of 20 h at ambient temperature produced a small amount of species **4** and **5**, respectively). Then compound **2** (15 mg, 0.039 mmol) was added in three portions as a solid. An immediate color change was observed, and after 15 min, a clear lemon-yellow solution was obtained. Evacuation to dryness gave a yellow residue, the proton NMR spectrum of which showed an approximate 1:1 molar mixture of species **4** and **5**.

(iii) Reaction of 3(I)$_2$ with Sodium Naphthalide. Sodium naphthalide (0.55 mmol, 9.0 mL of a solution prepared from the reaction of sodium (42 mg) with naphthalene (235 mg) in 30 mL of THF for 6 h with stirring) was added slowly via a syringe to a stirred suspension of **3**(I)$_2$ (100 mg, 0.09 mmol) in THF (15 mL). A clear greenish orange solution resulted; after 15 min this was evacuated to dryness, and the residue triturated with ether (3 × 5 mL) to extract the organometallic product together with naphthalene, leaving behind NaI. The combined extracts were passed through a disk (1.5 cm thick) of alumina (neutral, ACT III). A greenish impurity and naphthalene were eluted with ether (20 mL), followed by the product with CH_3CN (15 mL) as an orange solution, from which was obtained the monomethylation product [Cp*Ru{η^3-S(CH_2)$_2$S(CH_2)$_2$SMe}] (**8**) (40 mg, 53%).

Data for 8: ^{1}H NMR (δ, CD_3CN): 2.74−2.69 (6-line m, 1H, SC*H*$_2$), 2.23−2.08 (unres. m, 5H, SC*H*$_2$), 2.06 (s, 3H, SC*H*$_3$), 1.68 (s, 15H, C$_5$*Me*$_5$), 1.63−1.54 (9-line m, 2H, SC*H*$_2$). ^{13}C NMR (δ, CD_3CN): 86.1 (*C*$_5$Me$_5$), 45.7, 38.3, 33.2, 25.7 (*C*H$_2$), 17.4 (*C*H$_3$), 9.9 (C$_5$*Me*$_5$). FAB$^+$ MS: *m/z* 404 [M]$^+$. Anal. Calcd (found) for **8** ≡ ($C_{15}H_{26}IRuS_3$): C, 44.6 (45.0); H, 6.5 (6.4); S, 23.8 (24.1).

(iv) Reaction of 3(PF$_6$)$_2$ with Tri(*n*-butyl)tin Hydride. To a stirred dark red solution of **3**(PF$_6$)$_2$ (15 mg, 0.014 mmol) in CH_3CN (5 mL) was injected 7.5 μL (0.028 mmol) of ^{n}Bu$_3$SnH in the dark. The solution rapidly turned yellow in 5 min, but was left stirring for 30 min before evacuation to dryness to give a yellow oil of **9**(PF$_6$). Extraction with ether (3 × 2 mL) gave a yellow solution and some red residual solids (1 mg) consisting of unreacted **3**(PF$_6$)$_2$. The yellow solution was concentrated and kept at −30 °C. As the solution almost "dried out", orange crystalline solids of [Cp*Ru{μ-η^1-η^3-MeS(CH_2)$_2$S-(CH_2)$_2$S-}Sn(*n*-butyl)$_3$]PF$_6$, **9**(PF$_6$) (17 mg, 79% yield), were obtained after 6 days.

Data for 9(PF$_6$): ^{1}H NMR (δ, CD_3CN): 2.59 (cm unres, 2H, SC*H*$_2$), 2.25 (cm unres, 6H, SC*H*$_2$ + SC*H*$_3$), 1.72 (s br, 15H, C$_5$*Me*$_5$), 1.69−1.58 (8-line m, 6H, SnC*H*$_2$ + SC*H*$_2$), 1.43−1.28 (7-line m, 12H, SnCH$_2$(C*H*$_2$)$_2$ + SC*H*$_2$), 0.93 (t, *J* = 7 Hz, 9H, SnCH$_2$(CH$_2$)$_2$C*H*$_3$). ^{13}C NMR (δ, CD_3CN): 88.4 (s br, *C*$_5$Me$_5$), 40.8 (br, apparently an unresolved cluster of peaks) and 32.1 (*C*H$_2$), 29.0 (t, J_{Sn-C} = 20 Hz, SnCH$_2$*C*$_\beta$H$_2$), 27.6 (t, J_{Sn-C} = 69 Hz, Sn(CH$_2$)$_2$*C*$_\gamma$H$_2$), 16.2 (t, $J_{119/117Sn-C}$ = 321/305 Hz, Sn*C*$_\alpha$H$_2$), 13.7 (Sn(CH$_2$)$_3$*C*H$_3$), 10.0 (C$_5$*Me*$_5$). The observation of only four ^{13}C signals, three for CH_2 groups and one for CH_3, for the ^{n}Bu$_3$Sn moiety suggests the presence of equivalent *n*-Bu chains in solution due to ease of rotation along the S−Sn bond. The coupling constants J(^{117,119}Sn−C) for C$_{\alpha-\gamma}$ are in the range of the reported values for *n*-Bu groups.[18] FAB$^+$ MS: *m/z* 693 [M − PF$_6$]$^+$. FAB$^-$ MS: *m/z* 145 [PF$_6$]$^-$. Anal. Calcd (found) for **9**(PF$_6$) ≡ ($C_{27}H_{53}F_6PRuS_3Sn$): C, 38.7 (38.5); H, 6.4 (6.1); S, 11.5 (11.4).

(e) Reaction of 8 with MeI. To a stirred orange solution of **8** (15 mg, 0.04 mmol) in CH_3CN (8 mL) was injected MeI (20 μL, 0.32 mmol). The solution rapidly turned yellow, but was left stirring for 3 h before evacuation to dryness to give a yellow oil of **4**(I). This was treated with excess NH_4PF_6 (15 mg, 0.09 mmol) in CH_3CN (5 mL), and after stirring for 30 min the reaction mixture was evacuated to dryness. The product was extracted with CH_2Cl_2 (3 × 1 mL) and filtered through a glass sinter (Por. 4). Addition of ether to the yellow filtrate gave **4**(PF$_6$) (15 mg, 74%) as a yellow crystalline solid after 24 h at −30 °C. Its ^{1}H NMR spectrum matches that of **4**(I) given in section b(i). FAB$^+$ MS: *m/z* 419 [M − PF$_6$]$^+$. FAB$^-$ MS: *m/z* 145 [PF$_6$]$^-$. Anal. Calcd (found) for **4**(PF$_6$) ≡ ($C_{16}H_{29}F_6PRuS_3$): C, 34.1 (34.3); H, 5.2 (5.1); S, 17.1 (16.8).

X-ray Crystallography. X-ray data were collected on a Bruker AXS SMART CCD diffractometer, using Mo Kα radiation. The program SMART[19] was used for collecting frames of data, indexing reflection, and determination of lattice parameter, SAINT[19] for integration of the intensity of reflections, scaling, and correction of Lorentz and polarization effects, SADABS[20] for absorption correction, and SHELXTL[21] for space group and structure determination and least-squares refinements on F^2.

Experimental details together with a table of selected crystallographic data and refinement details are given in Table S1 (see Supporting Information).

Results and Discussion

Products and Reaction Pathways. Reactions of 2. (i) With Alkylating Reagents. Complex **2** underwent a facile reaction with two or more molar equivalents of the methylating agents, MeI or (Me$_3$O)BF$_4$, giving the respective salts of the S−S coupled complex [{Cp*Ru^{II}}$_2${μ-η^6-(S(CH_2)$_2$S(CH_2)$_2$SMe)$_2$}]$^{2+}$ (**3**) as the predominant product in dark red crystalline form. A similar reaction was obtained with ethyl iodide, giving dark red microcrystals of [{Cp*Ru^{II}}$_2${μ-η^6-(S(CH_2)$_2$S-(CH_2)$_2$SEt)$_2$}](PF$_6$)$_2$, **3$_{Et}$**(PF$_6$)$_2$, in 59% yield, after metathesis with NH_4PF_6 (see Supporting Information). A minor product, [Cp*Ru^{II}{η^3-S(CH_2CH_2SMe)$_2$}]I, **4**(I), was obtained when MeI was used, but was nondetectable in the reaction with (Me$_3$O)BF$_4$.

The equal effectiveness of MeI or (Me$_3$O)BF$_4$ in the transformation suggests that the reaction must have been initiated by electrophilic attack of Me$^+$ on a thiolate sulfur of **2**. This would generate racemic Ru(III) intermediates (*R*)-**3A′** and (*S*)-**3A′**.[22] An *internal electron transfer* (IET) in these then leads to the respective cationic Ru(II) sulfur-centered radicals (*R*)-**3A** and (*S*)-**3A**; coupling of these thiyl radicals would then give two pairs of S−S bonded dinuclear diastereomers (Scheme 2). The ^{1}H NMR spectral evidence is consistent with the presence of these diastereomeric pairs (discussed below), although only the *RS*- and *SR*-enantiomeric pair of species **3** has been crystallized out and hence characterized crystallographically.

To confirm the radical nature of this reaction, **2** was allowed to react with the methylating reagents in the presence of acrylonitrile, as it has been established that thiyl radicals add readily to olefins,[23] and strongly electrophilic alkenes such as AN have been demonstrated to be particularly effectively, reacting readily

(18) (a) Mitchell, T. N. *J. Organomet. Chem*. **1973**, *59*, 189. (b) Singh, G. *J. Organomet. Chem*. **1975**, *99*, 251.

(19) *SMART* & *SAINT* Software Reference manuals, Version 6.22; Bruker AXS Analytic X-Ray Systems, Inc.: Madison, WI, 2000.

(20) Sheldrick, G. M. *SADABS*, Software for Empirical Absorption Correction; University of Göttingen: Germany, 2000.

(21) *SHELXTL* Reference Manual, Version 5.1; Bruker AXS, Analytic X-Ray Systems, Inc.: Madison, WI, 1997.

(22) Specifications of chirality follow the widely accepted *R* and *S* conventions for tetrahedral compounds, developed by Cahn, Ingold, and Prelog (Cahn, R. S.; Ingold, C.; Prelog, V. *Angew. Chem., Int. Ed. Engl*. **1966**, *5*, 385) and the priority convention adopted for organometallic complexes (Stanley, K.; Baird, M. C. *J. Am Chem. Soc*. **1975**, *97*, 6598).

(23) (a) Walling, C.; Helmreich, W. *J. Am. Chem. Soc*. **1959**, *81*, 1144. (b) Chatgilialoglu, C.; Bertrand, M. P.; Ferreri, C. In ref 16a, Chapter 11, p 311, and references therein.

Scheme 2. Me^+ Alkylation

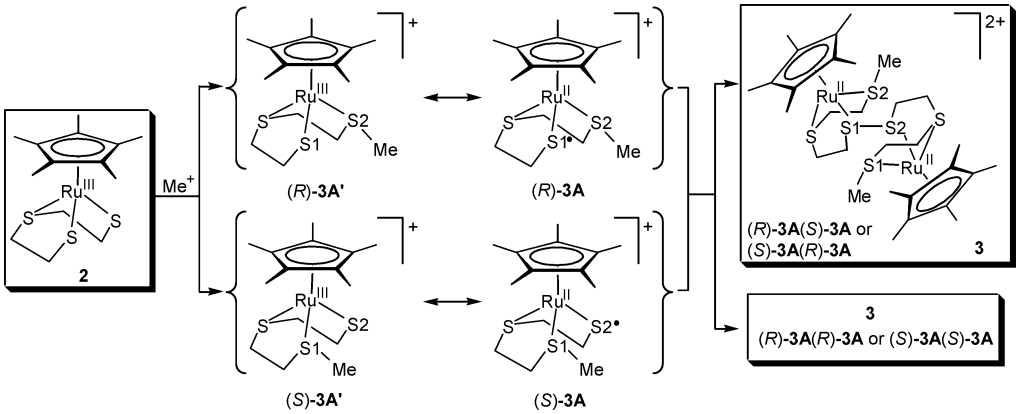

Scheme 3. Products with Isolated Yields (%) in the Presence of CH_2=CHCN (AN)

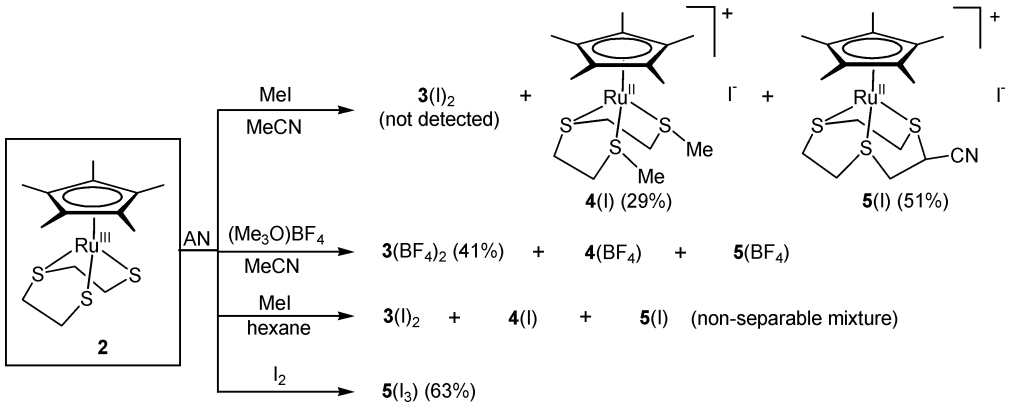

Scheme 4. Redox Interaction between 2 and I_2

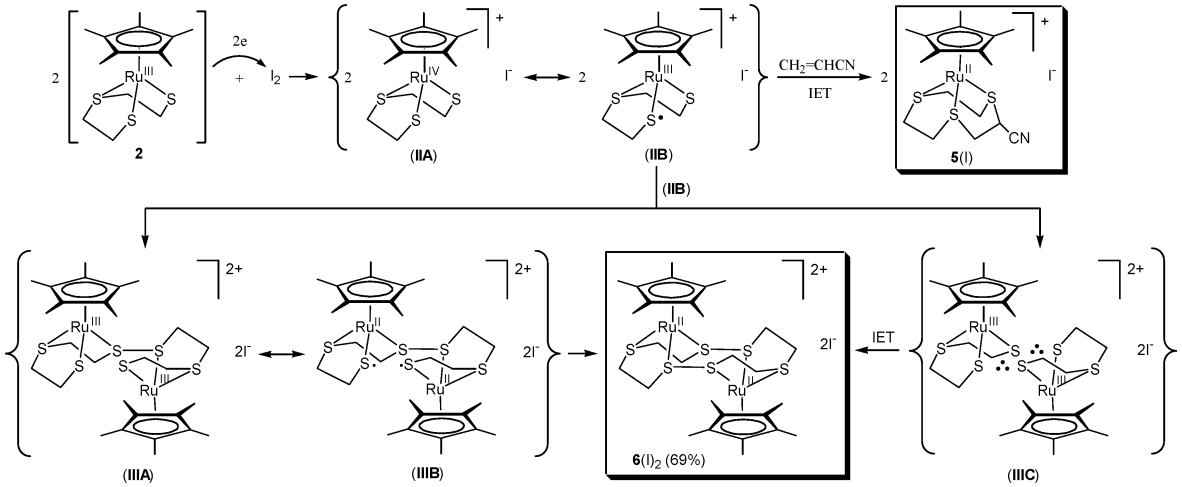

even with non-carbon radicals.[24] In the presence of a 10-fold excess of AN, markedly different product compositions were obtained, as summarized in Scheme 3. It was observed that the reaction with MeI in MeCN gave a homogeneous product solution, from which **5**(I) was isolated in 51% yield together with **4**(I) in ca. 29% yield, but with no detectable sign of species **3**. Yet, with substituting $(Me_3O)BF_4$ for MeI as alkylating agent, a substantial amount of **3**$(BF_4)_2$ was obtained (41% yield) in addition to species **4** and **5** in 1:1 molar proportion. Likewise, the same reaction with MeI in *hexane* gave a precipitate consisting of the iodide salts of *all three* species. Taken together, these three observations indicated that in the presence of AN species **3** was obtained from reactions with MeI or $(Me_3O)BF_4$. The apparently incongruent finding of the absence of **3** in the "MeI/MeCN" reaction is related to (i) the ability of **3** to react with **2** (rapidly in the presence of MeI/AN) to give species **4** and **5** (refer to section d(ii) of Experimental Section), but slowly in the absence of MeI/AN to give species **7** (refer to section d(i) of Experimental Section)), and (ii) the much faster relative reaction rate of (Me_3O)-BF_4 versus MeI (refer to section a(iii) of Experimental

(24) See recent papers and references therein: (a) Busfield, W. K.; Jenkins, I. D.; Monteiro, M. J. *Aust. J. Chem.* **1997**, *50*, 1. (b) Dondi, D.; Fagnoni, M.; Molinari, A.; Maldotti, A.; Albini, A. *Chem. Eur. J.* **2004**, *10*, 142.

Chart 1. Some RS−SR Coupled Species

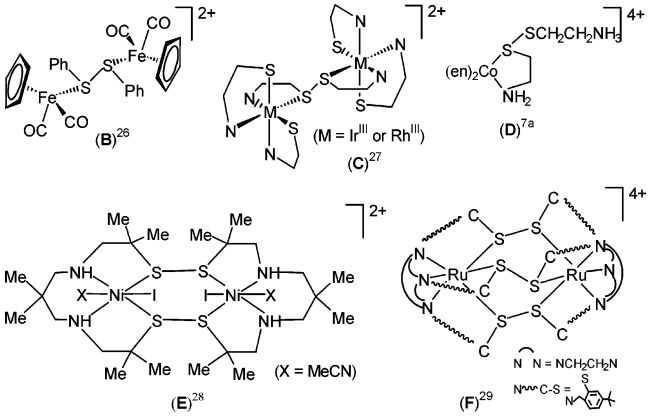

Section), resulting in a rapid depletion of **2**, thus leaving the bulk of the primary product **3** intact. In the "MeI/AN/hexane" reaction, it was the heterogeneous nature of the insoluble product mixture that had impeded the interaction of **2** and **3**.

(ii) With I_2. Species **5**, as its triiodide salt, was the sole product (63% isolated yield) from the reaction of **2** with I_2 in the presence of AN. In the absence of AN, an instantaneous reaction of **2** with I_2 led to the isolation of $[\{Cp^*Ru^{II}\}_2\{\mu\text{-}\eta^6\text{-}(S(CH_2CH_2S)_2)_2\}](I_3)_2$, **6**$(I_3)_2$, in 69% yield. These results are consistent with mechanistic pathways proposed in Scheme 4. The transformations are envisaged to go via a Ru(IV) species **IIA** (supported by electrochemical experiments), which undergoes intramolecular electron rearrangement to generate a Ru(III) S-centered radical **IIB**. In the *presence* of AN, the S-centered radical **IIB** is effectively trapped to form the AN adduct **5**. In the *absence* of AN, **IIB** dimerizes to form **IIIA**. A repeat intramolecular electron arrangement then gives the Ru(II)−Ru(II) diradical **IIIB**, which undergoes a second S−S coupling to give species **6**. Alternatively, twice coupling of the S radical of **IIB** with a lone pair on the thiolate S of a second unit of the same moiety would generate simultaneously two 2c/3e S−S bonds forming species **IIIC**. Such $(\sigma)^2(\sigma^*)^1$ odd-electron bonds are a common type of bond in heteroatom-centered radicals and radical ions.[25] The higher-energy electron in the σ^* orbital of this bond will readily be transferred to the Ru centers, giving the Ru(II)−Ru(II) species **6**. Complex **6** thus arises from an oxidation-induced S−S coupling, assisted with IET processes.

There are numerous examples of S−S[12−15] and RS−SR[26−29] coupled species (see Chart 1) generated by oxidation processes which can be metal- or sulfur-centered. However, as far as we are aware, an alkylation-induced IET process leading to thiolate sulfur coupling as in **3** has not been observed before.

Reactions of 3. The reactions of **3** with various substrates, viz. complex **2**, sodium naphthalide, and

Scheme 5. Reactions of 3 Involving S−S Cleavage, Showing Isolated Yields (%) of Products

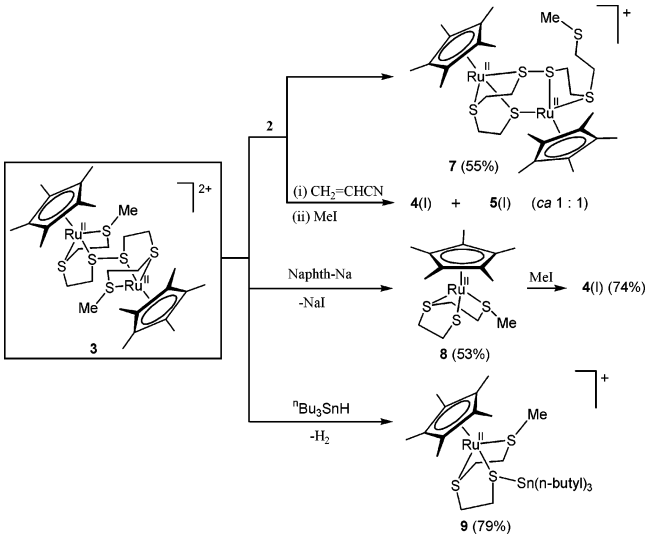

tributyl tin hydride, giving the products summarized in Scheme 5, can all be rationalized based on a facile homolytic dissociation of its S−S bond, (eq ii), which is deduced from electrochemical and VT-^{1}H NMR, EPR, and UV−vis spectral data (see below). Thus, as illustrated in Scheme 6, **3A** reacts as a radical initiator with ^{n}Bu$_3$SnH, an efficient H atom donor,[30] abstracting the radical ^{n}Bu$_3$Sn$^\bullet$ to form the RuSSnBu$_3$-containing complex **9** (route (a)); presumably the released H$^\bullet$ could have coupled to form H_2, since no other Ru-containing product was detected in the reaction.

In the reaction with sodium naphthalide, an electron reduces **3A**, generating complex **8**, which was isolated and readily alkylated to give **4** (route (b)). The interaction of **3A** with **2** had led to isolation of the dinuclear species **7**. The second-order kinetics of the reaction of **2** with **3**, first order in each reactant,[31] are consistent with a rapid mononuclear−dinuclear preequilibrium (eq ii), followed by a slower reaction of **3A** with **2** (route (c)). It

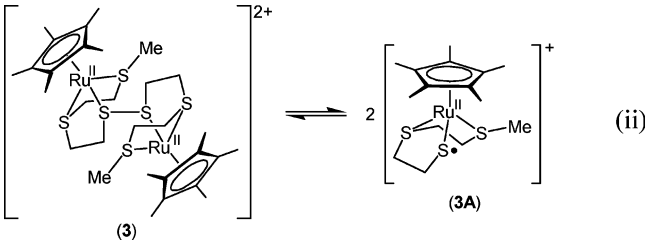

(ii)

is proposed that this involves the formation of an intermediate **IV** via coupling of the S-centered radical in **3A** and the S lone pair of **2** to give a S1∴S4 (2c/3e) disulfide bond, similar to that shown in **IIIC** in Scheme 4. As in **IIIC**, the transfer of the high-energy antibonding σ^* electron in this bond to Ru(III) results in a Ru(II) center and the S1−S4 bond; the remaining process required for the formation of **7** would involve either a concomitant or a subsequent intramolecular nucleophilic attack of thiolate S6 on *the other* Ru(II) center,

(25) Asmus K.-D.; Bonifačić, M. In ref 16a, Chapter 5, pp 141−191, and references therein.

(26) (a) Treichel, P. M.; Rosenhein, L. D.; Schmidt M. S. *Inorg. Chem.* **1983**, *22*, 3960. (b) Ashby, M. T.; Enemark, J. H.; Lichtenberger, D. L. *Inorg. Chem.* **1988**, *27*, 191.

(27) (a) Miyashita, Y.; Sakagami, N.; Yamada, Y.; Konno, T.; Okamoto, K. *Bull. Chem. Soc. Jpn*. **1998**, *71*, 2153. (b) Konno, T.; Miyashita, Y.; Okamoto, K. *Chem. Lett*. **1997**, 85.

(28) Fox, S.; Stibrany, R. T.; Potenza, J. A.; Knapp, S.; Schugar, H. J. *Inorg. Chem*. **2000**, *39*, 4950.

(29) Albela, B.; Bothe, E.; Brosch, O.; Mochizuki, K.; Weyhermüller, T.; Wieghardt, K. *Inorg. Chem*. **1999**, *38*, 5131, and references therein.

(30) Curran, D. P. In *Comprehensive Organic Synthesis*; Trost, B. M., Fleming, I., Eds.; Pergamon Press: Oxford, 1991; Vol. 4, Chapter 4.1, p 734, and references therein.

(31) Shin, R. Y. C.; Goh, L. Y. From work in progress.

Scheme 6. Reactions of 3A

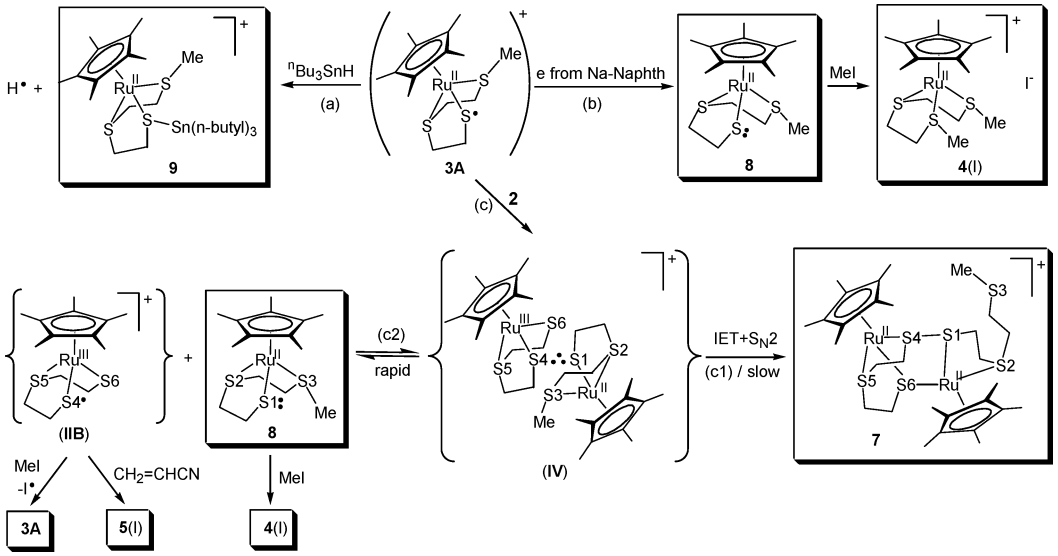

Scheme 7. Reaction of 3*, the "NS_2" Analogue of 3, with 2

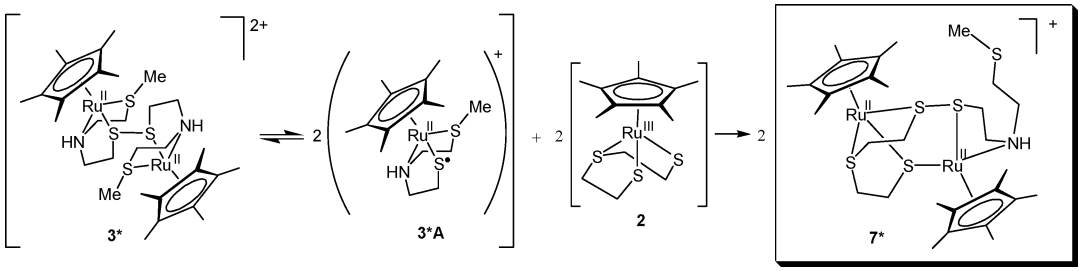

resulting in displacement of the ligated S3Me moiety, thus forming the $(CH_2)_2$S3Me pendant chain at S2 (route (c1)). Alternatively the weak S1∴S4 bond in **IV** could undergo reversible cleavage to the S4-centered radical **IIB** and species **8** with a lone pair electron at S1 (route (c2)); in essence this constitutes an inner-sphere transfer of an electron from **2** to **3A**. The interaction of **IIB** and **8** with AN and MeI, respectively, then gave the isolated species **5** and **4**. In the presence of MeI alone, it is highly likely that **IIB** will be converted via a radical pathway to species **3A**, which on dimerization will regenerate **3**.

We also considered two other probable pathways for the formation of **7**, viz. (a) a direct outer-sphere redox reaction between **2** and *dimeric* **3**, and (b) nucleophilic displacement processes. Pathway (a) was ruled out on the basis of the electrochemical data. Pathway (b) involving two S_N2 displacement processes—viz. a nucleophilic attack of **2** on a ligated SMe group in **3**, resulting in displacement/cleavage of Me and generation of a thiolate donor center, which then effects an intramolecular S_N2 displacement of *the other* SMe from its Ru center—would produce a molecule of **7** wherein both Ru centers originate from one and the same dinuclear molecule of **3**. To test this probability, complex **2** was reacted with the NS_2 analogue of **3**, viz. **3*** (Scheme 7). The isolated and structurally characterized product **7**[*31] illustrates definitively that such was not the case, vide infra, for the formation of **7**.

Electrochemical Studies. Cyclic voltammetric (CV) experiments indicated that **2** could be very easily oxidized at −0.55 V vs Fc/Fc^+ (Fc = ferrocene) and reduced at −1.57 V vs Fc/Fc^+. The voltammograms are illustrated in Figure 1. The couples are chemically reversible and involved one-electron, showing an anodic (E_p^{ox}) to cathodic (E_p^{red}) peak-to-peak separation (ΔE_p = 70 mV), which was close to that observed under identical conditions for the model one-electron system, Fc/Fc^+. The one-electron transfer was confirmed by controlled potential coulometry experiments during the oxidation process that led to the calculation of 0.91 electron transferred per molecule (i.e., $n = 1$), with the oxidized species ($\mathbf{2}^+$) (possibly a Ru(IV) species) being stable for at least several hours at low temperatures (233 K), but decomposing within 2−3 h at 293 K. $\mathbf{2}^+$ could also be further oxidized in a chemically irreversible multielectron process at ∼1.3 V vs Fc/Fc^+. The small reverse peak detected during CV experiments on the reduction process indicated that the one-electron-reduced species was only stable for a few seconds (Figure 1a).

The cyclic voltammetric behavior of **3** was analyzed by taking into consideration that **3** monomerizes into 2 mol of **3A** when dissolved in solution, according to eq ii. Thus, a solid sample of **3** that was dissolved in CH_2Cl_2 immediately formed a solution of **3A** and could be electrochemically reduced in a chemically reversible process at −0.75 V vs Fc/Fc^+ (Figure 1b). The ΔE_p value (75 mV) obtained during CV experiments was similar to that obtained for **2**. Controlled potential coulometry experiments indicated that 0.96 electron was transferred per molecule of **3A** (assuming **3** completely dissociates into 2 mol of **3A**) during the reduction process (i.e., $n = 1$) to form a species that was stable in

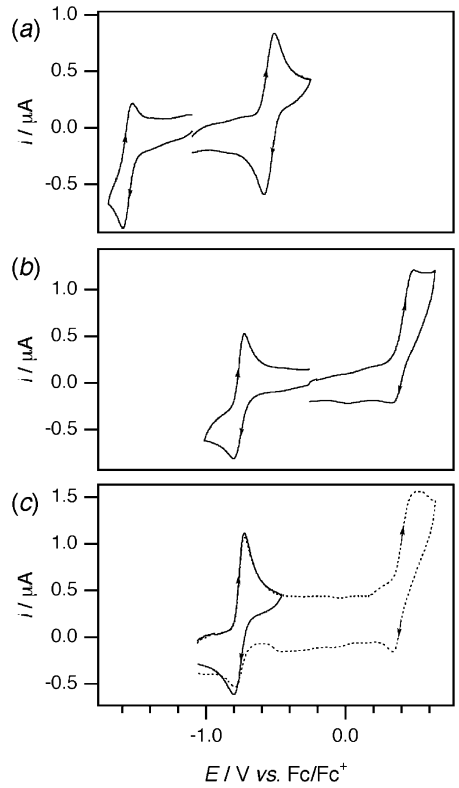

Figure 1. Cyclic voltammograms obtained with a 1 mm diameter GC working electrode at 100 mV s^{-1} in CH_2Cl_2 with 0.25 M Bu_4NPF_6 at 233 K: (a) 0.62 mM in **2**; (b) 0.50 mM in **3A**, based on a weighed sample of solid **3** dissociating into 2 mol of **3A** in solution through the equilibrium process in eq ii; (c) 0.69 mM in **8**.

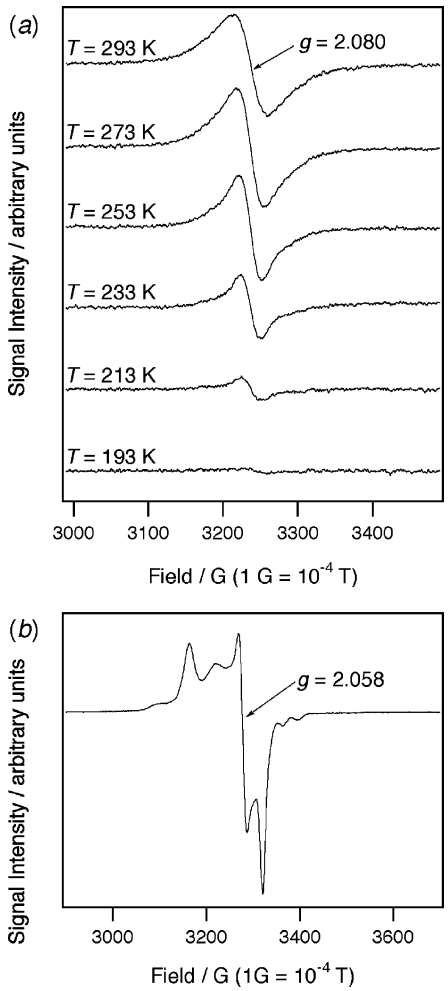

Figure 2. Continuous wave X-band EPR spectra: (a) 0.5 mM **3/3A** in CH_2Cl_2 obtained with microwave frequency = 9.43 (at 293 K) and microwave power = 2 mW; (b) 0.5 mM **2** in CH_2Cl_2 obtained at 10 K with microwave frequency = 9.442 GHz and microwave power = 0.2 μW.

solution for many hours in the absence of molecular oxygen. The starting material could be completely regenerated from the reduced species by applying a positive potential to the bulk reduced solutions. Solutions that contained **3A** could also be oxidized at approximately +0.4 V vs Fc/Fc^+ to form a species that appeared to react/decompose quickly, since only a small reverse peak was detected in the cyclic voltammogram.

Further convincing evidence that **3** dissociates into **3A** in solution came from cyclic voltammetric experiments performed on solutions of compound **8** (which is simply the one-electron-reduced form of **3A**) (Figure 1c) that appeared almost identical to that of solutions containing compound **3A** (Figure 1b), both showing a reversible couple at $E_{1/2} = -0.75$ V, and with coulometry experiments confirming the transfer of one electron per molecule. One notable (but expected) difference was that the starting form of **8** was *oxidized* at −0.75 V vs Fc/Fc^+, while the starting form of **3A** was *reduced* at −0.75 V, consistent with **3A** and **8** being a redox couple.

Wieghardt et al.[29] reported on the electrochemistry of a similar class of compounds, viz. mononuclear $[Ru^{III}L]$ and dinuclear $[Ru^{II}_2(L-L)](PF_6)_4$ (**F**). Interestingly, they also observed that the cyclic voltammetric behavior of the monomer and related dimer were identical. However, their electrochemical data were rationalized on the basis of a rapid reversible monomerization or dimerization reaction *following* electron transfer. Reversible dimerization of species formed during cyclic voltammetry experiments have been well documented in the literature, such as for thianthrene,[32] 9-substituted anthracenes,[33] 2,4,6-substituted phenols,[34] diphenylpolyenes,[35] aromatic esters,[36] and tris(dithiocarbamato)osmium.[37] Nevertheless, using a reversible monomerization/dimerization reaction post-electron transfer to account for the present CV data relies on the simultaneous occurrence of two unlikely scenarios. The first is that the monomer (**8**) and dimer (**3**) must be reduced or oxidized at identical potentials (even a small change in electrode potential of a few mV would be electrochemically detectable). The second coincidence is that the reduced form of the dimer must convert immediately into the neutral monomer following electron transfer and revert back to the dimer when the reverse potential is applied. The conversions must be

(32) (a) de Sorgo, M.; Wasserman, B.; Szwarc, M. *J. Phys. Chem.* **1972**, *76*, 3468. (b) Hübler, P.; Heinze, J. *Ber. Bunsen-Ges. Phys. Chem.* **1998**, *102*, 1506.
(33) (a) Hammerich, O.; Parker, V. D. *Acta Chem. Scand., Ser. B* **1981**, *35*, 341. (b) Parker, V. D. *Acta Chem. Scand., Ser. B* **1981**, *35*, 349. (c) Hammerich, O.; Parker, V. D. *Acta Chem. Scand., Ser. B* **1983**, *37*, 379. (d) Hammerich, O.; Parker, V. D. *Acta Chem. Scand., Ser. B* **1983**, *37*, 851.
(34) (a) Evans, D. H.; Jimenez, P. J.; Kelly, M. J. *J. Electroanal. Chem.* **1984**, *163*, 145. (b) Hapiot, P.; Pinson, J. *J. Electroanal. Chem.* **1993**, *362*, 257.
(35) Smie, A.; Heinze, J. *Angew. Chem., Int. Ed. Engl.* **1997**, *36*, 363.
(36) Webster, R. D. *J. Chem. Soc., Perkin Trans. 2* **1999**, 263.
(37) Wheeler, S. H.; Pignolet, L. H. *Inorg. Chem.* **1980**, *19*, 972.

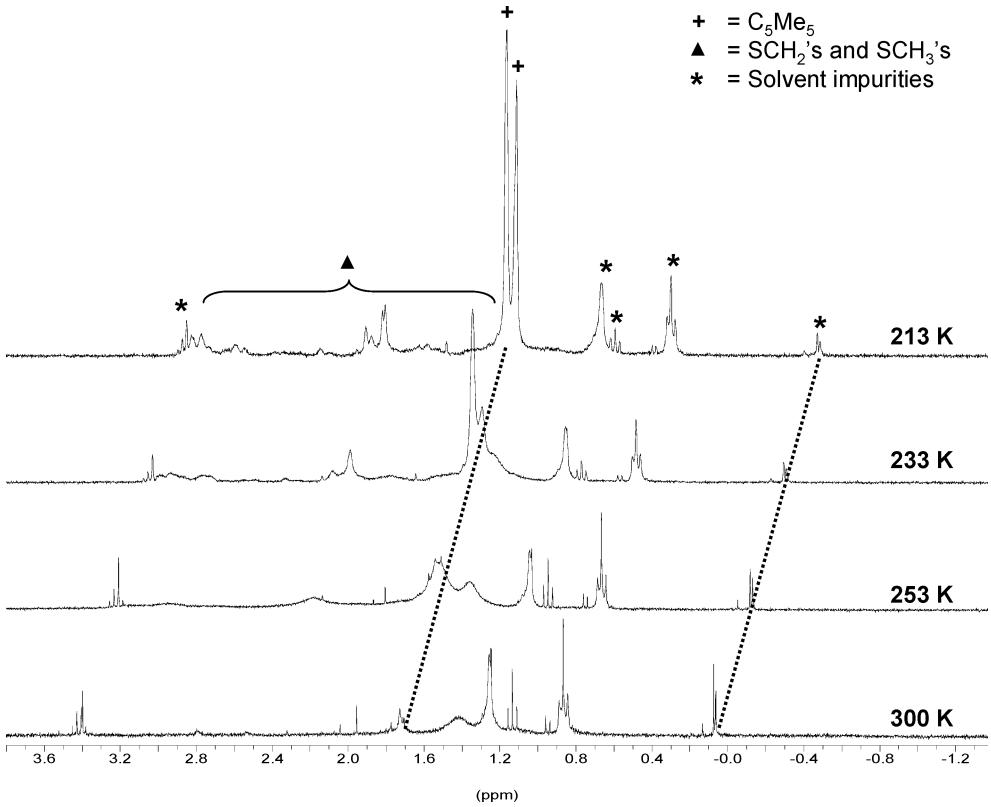

Figure 3. Variable-temperature ^{1}H NMR spectra of **3**$(PF_6)_2$ in CD_2Cl_2.

sufficiently fast in both directions to be indistinguishable from a conventional electron transfer step. In contrast, the equilibrium reaction pre-electron transfer proposed in eq ii relies on no special coincidences and is well supported by the spectroscopic data (see below).

EPR Studies. The monomer−dimer equilibrium (eq ii) was also supported by variable-temperature EPR experiments performed on solutions containing compound **3** (Figure 2a). Compound **3** (total valence electron count 36) should be diamagnetic, but a strong EPR signal was detected at $g = 2.080$ with $\Delta H_{pp} = 40$ G, which is consistent with the presence of the monomeric radical **3A**. As the temperature was decreased below 293 K, the intensity of the radical signal also decreased until it could not be detected at temperatures below 173 K (EPR experiments were performed at temperatures down to 10 K). The temperature-induced changes in the EPR spectra in Figure 2a were completely reversible. Such behavior is supportive of the equilibrium shifting toward the dimer (**3**) as the temperature is lowered, similar to that seen for the cation radical of thianthrene that forms a nonparamagnetic dimer at low temperatures.[32] The one-electron bulk electrochemical reduction of **3A** led directly to **8**, which is diamagnetic; therefore, no EPR spectrum was detected.

The room-temperature EPR spectrum of a CH_2Cl_2 solution of the 17e compound **2** displays an isotropic signal at $g = 2.007$ with a peak-to-peak separation (ΔH_{pp}) of 30 G. At low temperatures the EPR spectrum showed features typical of a ruthenium compound in a rhombic symmetry environment ($g_x = 2.132$, $g_y = 2.058$, and $g_z = 2.031$) (Figure 2b). Hyperfine coupling features were present in the low-temperature spectrum suggesting interactions of the unpaired electron with other nuclei, most likely protons in the bidentate sulfur ligands and suggesting substantial delocalization of the unpaired electron. Solutions of **2** that were exhaustively electrochemically oxidized by one electron at 0 V vs Fc/Fc^+ did not yield an EPR spectrum (even at 10 K).

VT ^{1}H NMR Spectral Study of 3. The ^{1}H NMR spectrum of **3**$(PF_6)_2$ in CD_2Cl_2 at ambient temperature exhibited three extremely broad bands centered at δ 1.73, 1.41, and 1.14. A variable-temperature study showed that at 253 K more distinct resonances began to appear, viz., two broad peaks assignable to Cp* ligands at δ 1.68 and 1.52 (relative intensity ca. 3:1) and two corresponding broad peaks assignable to SCH_2 groups centered at δ 2.33 and 3.11. The Cp* signals sharpened markedly below 233 K and appeared as sharp resonances (δ 1.62 and 1.57) of comparable relative intensities when the temperature was lowered to 193 K, while the SCH_2 resonances still remained as broad multiplets centered at δ 3.50, 3.08, 2.36, and 2.06, with two singlets at δ 2.30 and 2.29 assignable to SCH_3 groups.

Similar observations were made for the iodide salt of **3**. These spectral variations for the PF_6 salt are illustrated in Figure 3. This VT behavior is in agreement with the VT-EPR spectral data (Figure 2a), which showed the signal is insignificant at 213 K. The presence of what is essentially two sets of Cp* signals in the NMR spectra at 213 K and below is consistent with the existence of two diastereomeric (dinuclear) pairs, viz., *RR* + *SS* and *RS* + *SR*, which are in rapid equilibrium, hence the temperature dependence of their relative ratios.

UV−Vis Data. The spectra showed that (i) 10^{-4} M solutions of **3**$(PF_6)_2$ in MeCN did not obey Beer's law, with absorbances decreasing more than expected with dilution, indicating a mixture of species in solution, and

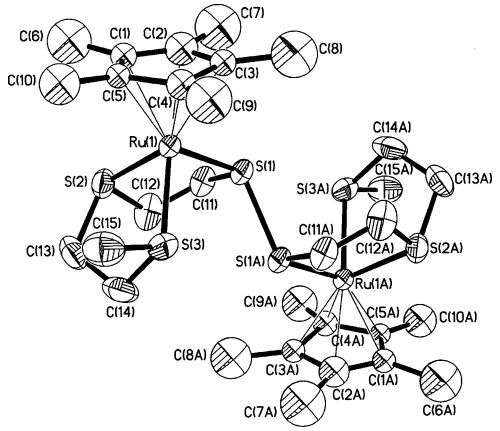

Figure 4. ORTEP plot for the molecular structure of $\mathbf{3}^{2+}$. Thermal ellipsoids are drawn at the 50% probability level.

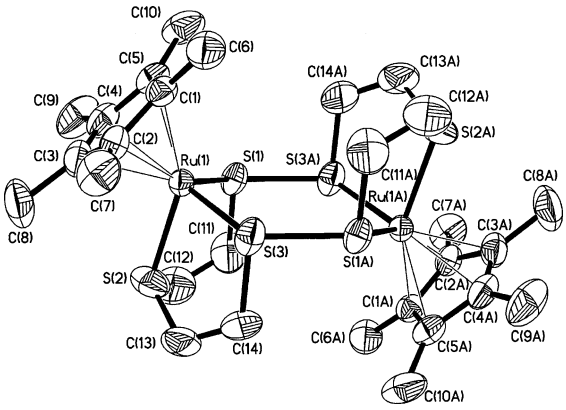

Figure 5. ORTEP plot for the molecular structure of $\mathbf{6}^{2+}$. Thermal ellipsoids are drawn at the 50% probability level.

(ii) there occurred a dramatic decrease of the absorptivity of the absorption band with an increase of temperature (shown in Figures S2 and S3 in Supporting Information). Such variations of solution electronic spectra of a species with concentration and with temperature were used elegantly by McLain as conclusive evidence for the dissociation of the M−M bond in $[CpCr(CO)_3]_2$.[38]

Crystal Structures. $(Cp^*Ru)_2(\mu\text{-}S_2)$ Complexes. The molecular structures of the disulfide diruthenium complexes **3**, **6**, and **7** are illustrated in Figures 4−6, and their significant metric data are given in Table 1. Complex **3** and its ethyl analogue $\mathbf{3_{Et}}$ (Figures 4 and S1 in Supporting Information) possess similar molecular structures, with a center of inversion at the midpoint of the S−S bond, which bridges two Cp*Ru units in *trans* η^1-η^1 configuration. The structure that shows *trans* orientation of the S-alkyl groups with respect to each other belongs to the (*RS*)- or (*SR*)-diastereomer; this has been found in the crystalline salts of the various anions studied, viz. PF_6^-, I_3^-, and BPh_4^-, though this may not be the only or the major diastereomer present in solution;[39] indeed, as discussed above, the VT ^{1}H NMR spectral scans of the iodide or PF_6 salts of **3** showed the presence of two sets of diastereomeric pairs.

The molecular structure of **6** (Figure 5) possesses a centrosymmetric Ru_2S_4 core, which is reminiscent of

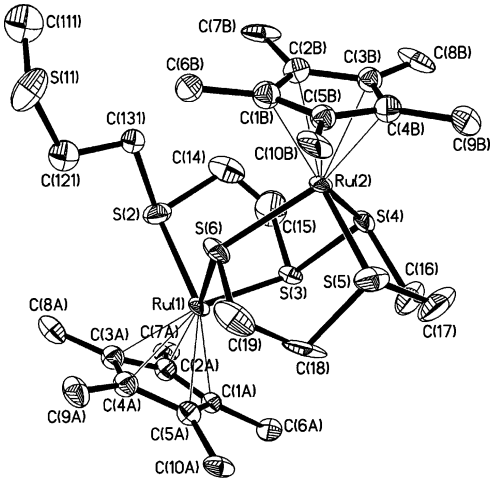

Figure 6. ORTEP plot for the molecular structure of $\mathbf{7}^{+}$. Thermal ellipsoids are drawn at the 50% probability level.

that in 1,4-$[(MeCp)Ru^{III}(PPh_3)]_2S_4$ (**G**) from Rauchfuss' work.[40] A six-membered ring is formed from two μ-η^1-η^1-S_2 moieties conjoined at two Ru centers in a *trans* configuration. The rings in both structures possess a chairlike conformation, which is less pronounced in **6**, in which the Ru atoms are only 0.5327 Å from the S_4 plane, the angle at the S−S hinge being 157.2°. Complex **G** possesses a larger S−Ru−S angle (106.42(5)° vs 100.5(1)° in **6**, and also a larger Ru−S−S angle (123.23(8) vs 110.1(1)°).

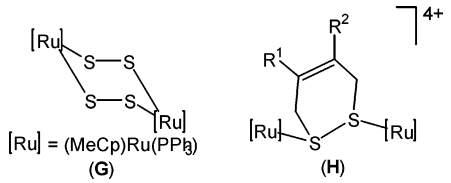

In the molecular structure of **7** (Figure 6), two Cp*Ru moieties are linked by a *cis* μ-η^1-η^1 S(3)−S(4) bridge and a μ-thiolate moiety (S(6)). It is seen that while S(4) and S(6) with S(5) are components of an intact tridentate tpdt on one Ru center, the tpdt ligand at the other Ru center has cleaved, being converted to an $S(3)CH_2$-$CH_2S(2)$ chelate with S(3) linked to S(4) and S(2) "alkylated" with a pendant $CH_2CH_2S(11)Me$ sidearm. As shown in Table 1, the Ru−S(thioether) bonds (Ru(1)−S(2) and Ru(2)−S(5)) are ca. 0.1 Å shorter than the bridging bonds Ru(1)−S(6) and Ru(2)−S(6).

The S−S distances of **3**, **6**, and **7** (range 2.160(2)−2.330(5) Å) are very close to values reported by Wieghardt for the tris *cis* η^1-η^1-S_2 bridged Ru(II)SSRu(II) complex **G** (2.198(1)−2.2152(7) Å);[29] these distances are longer than those found in the "inorganic" (μ-S_2) cores of Ru_2(III,III) complexes obtained by Taube,[12] Rauchfuss,[13] and Sellmann[14] (range 1.962(4)−2.014(1) Å), as well as in the (μ-SR_2) cores of Matsumoto's Ru_2(III,III) complexes of type **H** (range 2.093(5)−2.164(5) Å).[41] The elongation of the S−S bond in the Ru_2(II,II) cores is in agreement with the π-MO description of the RuSSRu

(38) McLain, S. J. *J. Am. Chem. Soc.* **1988**, *110*, 643.
(39) Faller, J. W.; Parr, J.; Lavoie, A. R. *New J. Chem.* **2003**, *27*, 899.
(40) Amarasekera, J.; Rauchfuss, T. B.; Rheingold, A. L. *Inorg. Chem.* **1987**, *26*, 2017.
(41) (a) Matsumoto, K.; Matsumoto, T.; Kawano, M.; Ohnuki, H.; Shichi, Y.; Nishide, T.; Sato, T. *J. Am. Chem. Soc.* **1996**, *118*, 3597. (b) Matsumoto, K.; Sugiyama, H. *Acc. Chem. Res.* **2002**, *35*, 915, and references therein.

Table 1. Selected Bond Lengths (Å) and Angles (deg) of the S−S Bridged Dinuclear Complexes

3$(I)_2$[a]		**3**$_{Et}(PF_6)_2$[a]		**6**$(I_3)_2$[b]		**7**(I)	
Ru(1)−S(1)[c]	2.2813(17)	Ru(1)−S(1)[c]	2.2831(16)	Ru(1)−S(1)[c]	2.2977(15)	Ru(1)−S(3)[c]	2.240(3)
Ru(1)−S(2)	2.3261(18)	Ru(1)−S(2)	2.3276(16)	Ru(1)−S(2)	2.3095(18)	Ru(2)−S(4)[c]	2.237(4)
Ru(1)−S(3)	2.3702(19)	Ru(1)−S(3)	2.3474(17)	Ru(1)−S(3)[c]	2.2942(16)	Ru(1)−S(2)	2.338(4)
S(1)−S(1A)	2.194(3)	S(1)−S(1A)	2.221(3)	S(1)−S(3A)	2.160(2)	Ru(1)−S(6)	2.436(3)
				S(3)−S(1A)	2.160(2)	Ru(2)−S(5)	2.291(4)
						Ru(2)−S(6)	2.411(3)
						S(3)−S(4)	2.330(5)
S(1)−Ru(1)−S(2)	86.96(6)	S(1)−Ru(1)−S(2)	86.54(6)	S(1)−Ru(1)−S(2)	85.58(7)	S(2)−Ru(1)−S(3)	86.33(14)
S(1)−Ru(1)−S(3)	95.9(6)	S(1)−Ru(1)−S(3)	109.30(6)	S(1)−Ru(1)−S(3)	106.42(5)	S(2)−Ru(1)−S(6)	89.37(14)
S(2)−Ru(1)−S(3)	86.1(6)	S(2)−Ru(1)−S(3)	85.12(6)	S(2)−Ru(1)−S(3)	86.34(7)	S(3)−Ru(1)−S(6)	95.44(12)
				Ru(1)−S(1)−S(3A)	123.23(8)	S(4)−Ru(2)−S(5)	87.27(15)
						S(4)−Ru(2)−S(6)	95.92(12)
						S(5)−Ru(2)−S(6)	87.33(14)
						Ru(1)−S(6)−Ru(2)	119.00(14)

[a] The molecule possesses a center of inversion. [b] The molecule possesses a plane of symmetry. [c] Pertaining to the RuSSRu moiety.

Table 2. Selected Bond Lengths (Å) and Angles (deg) of Mononuclear Complexes

4(PF_6)		**5**(I)		**8**		**9**(PF_6)	
Ru(1)−S(1)	2.3383(6)	Ru(1)−S(2)	2.2979(17)	Ru(1)−S(1)	2.415(3)	Ru(1)−S(1)	2.3539(14)
Ru(1)−S(2)	2.3280(6)	Ru(1)−S(2A)	2.2979(17)	Ru(1)−S(2)	2.341(3)	Ru(1)−S(2)	2.3218(14)
Ru(1)−S(3)	2.3519(6)	Ru(1)−S(3)	2.309(2)	Ru(1)−S(3)	2.269(3)	Ru(1)−S(3)	2.3939(14)
S(1)−C(11)	1.809(3)	C(4)−N(3)	1.229(16)	S(1)−C(11)	1.80(2)	Sn(1)−S(3)	2.5179(14)
S(3)−C(16)	1.806(3)	C(2A)-C(4)	1.44(2)				
S(1)−Ru(1)−S(2)	86.09(2)	S(2)−Ru(1)−S(2A)	86.75(9)	S(1)−Ru(1)−S(2)	85.22(9)	S(1)−Ru(1)−S(2)	86.54(5)
S(1)−Ru(1)−S(3)	93.62(2)	S(2)−Ru(1)−S(3)	87.58(6)	S(1)−Ru(1)−S(3)	95.77(12)	S(1)−Ru(1)−S(3)	89.26(5)
S(2)−Ru(1)−S(3)	86.40(2)	S(2A)-Ru(1)−S(3)	87.58(6)	S(2)−Ru(1)−S(3)	86.82(10)	S(2)−Ru(1)−S(3)	85.22(5)
		S(2)−C(2A)−C(4)	103.4(9)				
		C(2A)-C(4)−N(3)	175.1(13)				
		C(3A)-C(2A)-C(4)	115.8(12)				

core by Elder,[12b] Sellmann,[14] and San Filippo,[42] who showed that the two unpaired electrons of the two Ru(III) atoms occupy a distinct π-MO as an electron pair. With additional electrons entering antibonding orbitals, the bond order of the bond decreases, resulting in bond lengthening. It is clear that most of these S−S distances are longer than the normal single bond (cf. S−S single bond = 2.04−2.10 Å in S_8[43] and 2.038 Å in dimethyl disulfanes[44]).

The Ru−S distances in **3**, **6**, and **7** are comparable to those in the Ru_2(II,II) complex **F** (av 2.3287(6) Å)[29] and longer than those in Ru_2(III,III) complexes of type **A** (av 2.193−2.243 Å). A close comparison of the cyclic Ru_2S_4 core of **6** with that of [1,4-[{(MeCp)Ru^{III}(PPh3)}$_2$(μ-S_2)$_2$] (**G**) showed that their Ru−S distances are very similar, averaging 2.2959(16) and 2.295 Å, respectively.[40] Rauchfuss had rationalized the generally observed longer Ru−S distances in Ru_2(II,II) complexes on the perceived strong π-donor capability of the π-S_2 ligand based on spectroscopic, electrochemical, and crystallographic data.[13b]

(b) Mononuclear Complexes. The ORTEP diagrams of the mononuclear complexes **4**, **5**, **8**, and **9** are illustrated in Figures 7−10, respectively, and their metric data given in Table 2. The molecular structure of **4** shows a monocationic bis-S-methylated Ru(II) derivative of **2**. The Ru−S(Me) distances are longer than the distance of Ru to the central S atom of the ligand. They all fall within the range (2.302(2)−2.384(2) Å) of Ru−S(thioether) in **3**, **3**$_{Et}$, and previously reported (arene)Ru(II) complexes.[4] As in **3** and **3**$_{Et}$, the "open" S(1)−Ru(1)−S(3) angle is larger than the other two S−Ru−S angles by 7−9°.

The X-ray diffraction analyses of complexes **5**, **8**, and **9** show the presence of racemic mixtures. The molecular

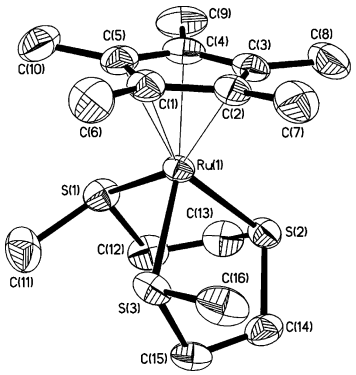

Figure 7. ORTEP plot for the molecular structure of $\mathbf{4}^+$. Thermal ellipsoids are drawn at the 50% probability level.

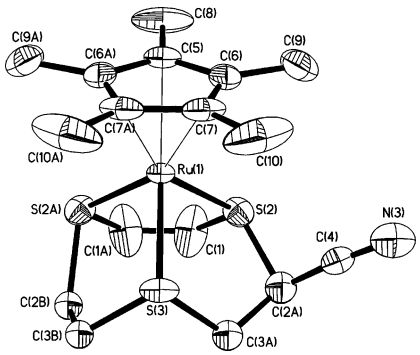

Figure 8. ORTEP plot for the molecular structure of $\mathbf{5}^+$. Thermal ellipsoids are drawn at the 50% probability level.

(42) Kim, S.; Otterbein, E. S.; Rava, R. P.; Isied, S. S.; San Filippo, J., Jr.; Waszcyak, J. V. *J. Am. Chem. Soc.* **1983**, *105*, 336.

(43) Pauling, L. In *The Nature Of The Chemical Bond,* 3rd ed.; Cornell University Press: Oxford, 1960; Chapter 7, p 224.

(44) Meyer, B. *Chem. Rev*. **1976**, *76*, 367, and references therein.

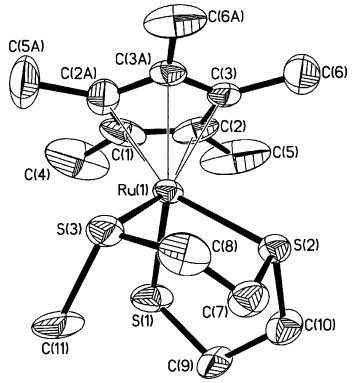

Figure 9. ORTEP plot for the molecular structure of **8**. Thermal ellipsoids are drawn at the 50% probability level.

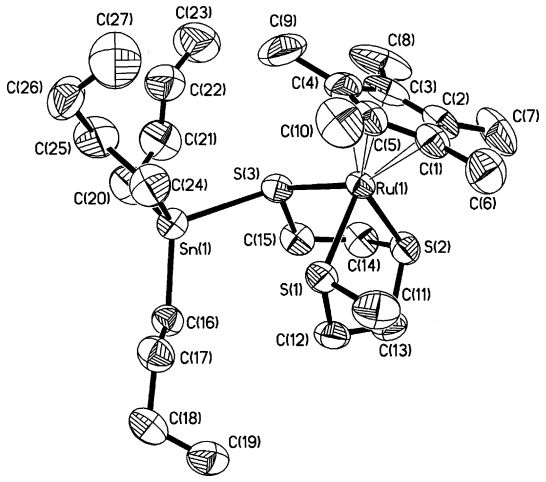

Figure 10. ORTEP plot for the molecular structure of $\mathbf{9}^+$. Thermal ellipsoids are drawn at the 50% probability level.

structure of **5** contains a Ru(II) center coordinated to η^5-Cp* and a η^3-1,4,7-trithiacyclononane (9S3) ligand carrying a cyano substituent at one of its methylene carbons; such a cyano-9S3 ligand has not been previously reported. The "$S(CH_2)_2S$" moieties subtend angles at Ru equal to 87.58(6)° and 86.75(9)°. The CN substituent is orientated away from the Cp* ligand, with angles S(2)C(2A)C(4), C(3A)C(2A)C(4), and C(2A)C(4)N(3) being 103.4(9)°, 115.8(12)°, and 175.1(13)°, respectively.

The variation of Ru−S distances within each of the molecular structures increases in the order **5** < **4** < **9** ≪ **8**.

Summary

Alkylation of the *cis*-dithiolate complex [Cp*Ru^{III}(tpdt)] (**2**) resulted in alkylation at one thiolate center and S−S coupling at the other, generating a *trans*-μ-η^1-η^1-S_2 dinuclear complex **3**. Unlike in our previous studies with [(HMB)Ru^{II}(tpdt)] (**1**), the dialkylation mononuclear product **4** was only a minor product. Evidence for the involvement of Ru^{II} S-centered radicals formed by a thiolate alkylation-initiated IET process was provided using acrylonitrile as a radical trap to produce **5**, carrying a cyano-9S3 ligand. The formation of **4** was rationalized on the observed reversible homolytic cleavage of the S−S bond of **3**, based on a combination of electrochemical, EPR, UV−vis, and NMR spectral studies. This was supported by product studies related to several reactivity features of **3**, arising from its incumbent monomeric form (**3A**), viz. (i) electrochemical or chemical reduction to yield the mono-S-methylated mononuclear complex **8**, which on further methylation gave **4**, (ii) behavior as a radical initiator on $^nBu_3SnH$, generating a RuSn complex **9**, and (iii) coupling with **2** to form a S∴S bonded intermediate. The latter can undergo an IET with an S_N2 reaction to generate the S−S bonded complex **7**, or S∴S bond cleavage to form species **8**, **4**, and **5**, in the presence of MeI and AN. Additionally, it was found that **2** is very easily oxidized electrochemically to a Ru(IV) species, and chemically by iodine to yield a centrosymmetric complex **6** containing a cyclic $Ru^{II}(\mu\text{-}S_2)_2Ru^{II}$ core. Formation of the latter is postulated to occur via the initial Ru(IV) species, which subsequently undergoes an intramolecular electron rearrangement to produce a Ru(III) S-radical species, capable of twice S−S coupling to form **6** or reacting with AN to form **5**.

The facile alkylation-induced S−S bond coupling and the ease of reversible homolytic S−S bond scission appear to be unique to this Ru(III) system. It is conceivable that the internal electron transfers postulated in the transformations described are facilitated by the relatively higher stability of d^6-Ru(II) versus Ru(III) or Ru(IV) oxidation states.

Acknowledgment. We thank the National University of Singapore for Academic Research Fund Grants No. R14300135112 and R143000209112 to L.Y.G., research scholarships to R.Y.C.S. and M.E.T., Dr. S. H. Goh of the Forest Research Institute of Malaysia for helpful discussions, and Dr. L. L. Koh and Ms. G. K. Tan for technical assistance.

Supporting Information Available: X-ray crystallographic files in CIF format, experimental details, and crystallographic data and refinement details for the structure determinations of $\mathbf{3_{Et}}$ and **3**−**9** (Table S1); Table S2 for IR spectral data; Table S3 giving cyclic voltammetric data obtained for **2**, **3**, and **8**, and Table S4 giving data associated with controlled potential electrolysis experiments. (I) Experimental details for alkylation of **2** with EtI synthesis and characterization of $\mathbf{3_{Et}}$, ethyl analogue of **3**. (II) UV−vis spectral studies of **3**. Figure S1 showing the ORTEP diagram of $\mathbf{3_{Et}}$. Figures S2 and S3 showing variation of electronic spectra of solutions of **3** in MeOH with concentration and with temperature. This material is available free of charge via the Internet at http://pubs.acs.org.

OM049081O